Reconfigurable Fault-Tolerant Control System for a Segmented Reflector Telescope Testbed

YEVA KOMANDYAN, HELEN H. BOUSSALIS, JOSE D. COVARRUBIAS, KHOSROW RAD, DAVID-ROBERT GRAVES, ABDELBASSIT ALKHATIB
Department of Electrical Engineering
California State University, Los Angeles
5151 State University Dr. Los Angeles, CA 90032
UNITED STATES OF AMERICA
http://www.calstatela.edu/orgs/space

Abstract— This paper presents the research conducted at the NASA sponsored Structures, Pointing and Control Engineering (SPACE) laboratory in designing a decentralized reconfigurable control (DRC) system for a segmented reflector testbed. The objective of the DRC system is to develop controllers that can satisfy performance specifications in both normal and failure situations. This objective is accomplished by integrating a nominal controller with sensor fault detection and isolation (SFDI) and reconfigurable controllers. A centralized reconfigurable control system is rarely feasible in large-scale systems due to the large number of computational operations. However, by implementing a decentralized approach, the reconfigurable control system can be divided into a number of relatively small tasks that can be implemented by several processors working in parallel. Simulation and implementation results for the SFDI algorithm are presented. The objective of this research is broader in the sense that the methods and tools developed in this study shall be useful for and applicable to a wide variety of reconfigurable control applications.

Key Words: Decentralized Control, Fault Detection and Isolation, Reconfigurable Control, Luenberger Observer

1 Introduction

To meet the scientific objectives of NASA's ORIGINS program, the new infrared (IR) space observatory that will replace the Hubble Space Telescope after the end of its useful life will have to be cost-effective in design. It should feature excellent angular resolution, spectral coverage and sensitivity in the UV, visible and infrared regions. The James Webb Space Telescope (JWST), formerly known as Next Generation Space Telescope (NGST), with its large light-gathering mirror and superb resolution will be capable of detecting faint signals from the first billion years, the period when galaxies formed [1]. The JWST will be capable of detecting radiation whose wavelength lies in the range of 0.6 to 20 mm. Furthermore, the JWST must be able to see objects 400 times fainter than those currently studied with large ground-based infrared telescopes.

Future missions such as the JWST will employ segmented reflectors instead of a monolithic mirror mainly because of the size and weight limitations associated with the launch vehicles. Major difficulties are associated with this technique such as the ability to provide a phasing of the separate beams. This problem requires special consideration in the optical design so that the individual focal planes can be properly aligned. The different segments can be easily misaligned due to disturbances; therefore a controller is necessary for the shaping of the mirrors in order for the images to be reflected at the central panel. Another challenge in the integration of such advanced optical systems is the stringent requirements for the pointing of the telescope. More importantly it is critical for such a system to maintain its performance requirements during normal and anomalous situations, which is the concentration of this paper.

2 Testbed Description and Performance Requirements

2.1 The SPACE Testbed

The SPACE testbed shown in Fig. 1 emulates a Cassegrain telescope of 2.4-meter focal length with performance comparable to an actual space-borne system. The system's top-level requirements include figure maintenance of the primary mirror to within 1 micrometer RMS distortion with respect to a nominal shape of the primary mirror, and precision pointing with accuracy of 2 arc seconds [3]. The SPACE testbed consists of a primary mirror, a secondary mirror and a lightweight flexible truss structure. The primary mirror (mounted on the support truss) consists of seven hexagonal panels each having 101 cm in diameter. The six peripheral panels are actively controlled in the three degrees-of-freedom by 18 linear electromagnetic actuators (3 actuators per active panel), and the seventh panel is used as a reference. In addition, a set of 18 edge sensors are used to provide measurements of relative displacement and angle of the panels (3 sensors per active panel). The testbed's active secondary mirror is a six sided pyramidal mirror, used to reflect the light from the primary mirror to the focal plane in the central plane and it is attached to the primary by a tripod. The entire testbed is supported on a triangular isolation platform made of aluminum honeycomb core with stainless steel top and bottom skin.

The data acquisition system consists of a digital signal processor (DSP) (A Pentek 4285 with four Texas Instruments TMS320C40 processors) and Dual A/D and D/A converter package from Pentek. The data flow path originates at the sensors and transferred to the three DSPs. The DSPs generate output commands based on the control algorithm, which translate to forces for the segment actuators to achieve the desired alignment.

2.2 Requirements

In the future mission of a real segmented space telescope system the information from the far region in the space will be collected by the light that is hitting its

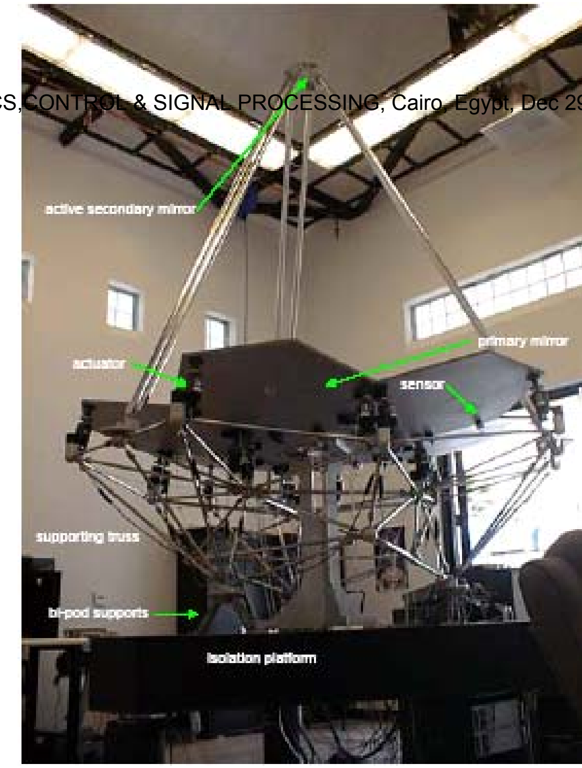

Fig. 1. The SPACE Testbed

primary mirror and then reflecting by its secondary mirror to a focal plane in a central panel. Therefore it is important for the primary mirror to behave as a desired single surface. The deviation of the primary mirror shape from its desired shape is characterized by the edge sensor outputs. In the test-bed, 6 shape error values for the 6 active panels are used to indicate how far the primary mirror is from its desired shape and are defined as:

$$S_{e_i} = \sqrt{\frac{\tilde{y}_i^T \tilde{y}_i}{3}} \quad i = 1, \ldots, 6 \tag{1}$$

where $\tilde{y}_i \in R^3$ is the i^{th} local output vector y_i of the active panel i after filtering measurement noises. Our objective is to reduce the effect of disturbances on the S_{e_i} values by 100:1 at steady state for both normal and sensor failure situations.

3 Decentralized Control

Decentralization is used to overcome the difficulties that arise due to the high dimensionality of some systems, where in centralized systems all the information and calculations take place at a single location. Some large physical systems such as power networks, traffic networks, ecological and economic systems are characterized by geographic separation providing motives for decentralization. The two main challenges associated with decentralized control of large scale systems are the problems associated with stability and controllability. The solution of the stabilization of decentralized control is based on the decentralization of the fixed modes as stated in Wang and Davidson [6].

The SPACE testbed under consideration consists of a large number of structural components as well as sensors and actuators leading to mathematical models that involve hundreds of states. Consequently, the design of control laws based on the conventional centralized approach becomes exceedingly difficult with the number of calculations that can be made in each operation cycle [8]. In addition, it is vulnerable to both a single point of failure and loss of computational and communicational abilities. As a result, the division of the control problem into a collective set of six smaller subsystems to control on a local level by set of decentralized controllers is a possible alternative to the centralized controller [9]. For control purposes the following state-space representation of the composite system is derived from (2) [5]:

$$\begin{aligned} \dot{x} &= Ax + Bu \\ y &= Cx \end{aligned} \qquad (2)$$

with decomposition

$$\begin{aligned} \dot{x}_i &= A_{ii}x_i + \sum_{1}^{6} A_{ii}x_i + B_{1i}u_i + B_{2i}d \\ y_i &= C_i x_i \end{aligned} \qquad (3)$$

and the isolated components are:

$$\begin{aligned} \dot{x}_i &= A_i x_i \\ where\ x_i &= \begin{bmatrix} \delta_i^T & \dot{\delta}_i^T \end{bmatrix} \end{aligned} \qquad (4)$$

In this case, a natural decentralization of the system is chosen by selecting one of the six peripheral segments of the primary mirror and its associated supporting structure as an isolated subsystem. Therefore, each subsystem is identified with three command inputs to the actuators and three outputs which are measured by the edge sensors. Local control algorithms are developed for each of the six isolated subsystems:

$$\begin{aligned} \dot{x}_i &= A_{ii}x_i + B_{1i}u_i + B_{2i}d \\ y_i &= C_i x_i \end{aligned} \qquad (5)$$

With decentralization, the control computation can be performed in parallel using the distributed control systems. Decentralization techniques are employed on the SPACE testbed for the development of control laws to accomplish vibration suppression, precision pointing and reflector shape control.

4 Fault-Tolerant Control System

4.1 Decentralized Sensor Fault Detection and Isolation

The design of a decentralized reconfigurable controller involves the development of fault detection and isolation as well as a reconfiguration scheme. The fault detection and isolation (FDI) process consists of two stages: residual generation and decision making. Figure 2 shows the structure of an FDI system. Inputs to actuators and outputs from sensors are processed to calculate the effect of a failure. The processed measurements which intuitively represent the error are called the residuals.

In order to generate such residuals, redundancies, physical or analytical, must be introduced in the system. Physical redundancies require extra components (such as sensors or actuators) to be added to the original system. The emphasis of this paper is on analytical redundancy, which is the basis for residual generation. In this section, the design of the FDI based on the Luenberger Observer method [5] is presented. The design steps of the DFDI system are:

1) Residual Generation – The DFDI scheme consists of N local units where each unit is responsible for sensor fault detection and isolation within the corresponding subsystem. Each of the local units consists of m_i banks of residual generators, where each bank is driven by all local inputs and one local output. A robust full state observer design is considered to generate the necessary m_i residuals. In practice it is desired to estimate the states of the system given by (2). State estimation can be accomplished by designing a generalized Luenberger observer with the following structure:

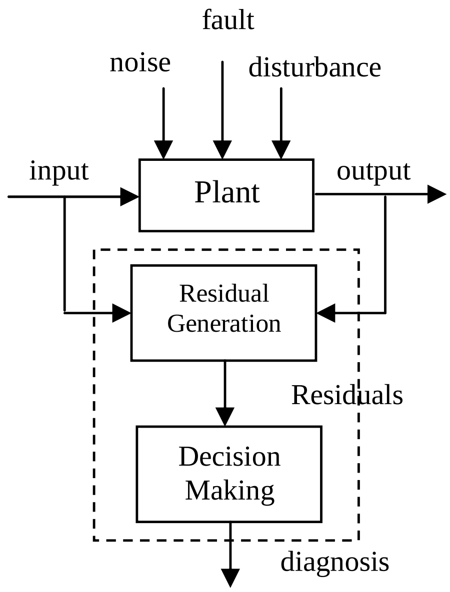

Fig. 2. General structure of SFDI scheme

$$\dot{\hat{x}}_i(t) = A_i\hat{x}_i(t) + B_i u_i(t) + L_i\left[y_i(t) - \hat{y}_i(t)\right]$$
$$\hat{y}_i(t) = C_i\hat{x}_i(t) \qquad (6)$$

where $\hat{x}$ is the state vector for the observer. Matrix L is a design parameter, which must be chosen such that $\hat{x} \to x \text{ as } t \to \infty$, thus $e_x = x - \hat{x}$ rapidly decays to zero. The dynamics of the error can be derived by subtracting (6) from (5), which yields the following:

$$\dot{e}_x = (A - LC)e_x - LFf_s \qquad (7)$$
$$e_y = Ce_x \qquad (8)$$

Given an observable subsystem, matrix L can be designed by placing the eigenvalues of $(A - LC)$ at any desired location such that the error signals exhibit the desired dynamics. Assuming that all eigenvalues have a negative real part ensures that the state error asymptotically decays to zero. The residual signal is defined by the output error $e_y = y - \hat{y}$, which can also be written as:

$$r = v(y - \hat{y}) \qquad (9)$$

Vector v is designed to minimize the effects of disturbance and noise in the system and maximize the effects of faults on the residual. The optimal vector v can be computed by using singular value decomposition.

2) Residual Evaluation – Each generated residual is tested for the likelihood of sensor faults. A decision about an existing sensor failure is made by comparing the absolute value of the residual with a preselected threshold value. The evaluation function is given by:

$$\theta = \| r(t) \|_2 = \sqrt{\int_0^\infty | r(\tau) |^2 \, d\tau} \qquad (10)$$

If the absolute value of the residual exceeds the threshold value, a sensor failure will be considered in the system. The threshold value is selected from experiments in order to reduce false alarms that can be generated from noises, modeling errors, subsystem interactions, and disturbances.

3) Sensor fault isolation - The location of the faulty sensor is the most important information required by the supervision system. For this reason, m_i banks of the residual generators are used in each of the N local units of the DFDI scheme. In this case, the m_i residual generators will respond differently according to the location of faulty sensor(s). These different responses are used to find the location of faulty sensor(s).
4) Fault Modeling – Many types of sensor faults such as sudden, slowly developing, intermittent, hard, or soft can occur and are usually described based on the time-behavior and magnitude. The effects of these different types of sensor faults on a system can be modeled as an unknown time-dependent vector added to the system output vector.

5 Simulation Results

Initially, six local passive H_∞ controllers were designed to control the position of the six active panels in the Matlab environment. The six local controllers guarantee the performance for the shape control of the primary mirror to within 1 micrometer RMS.

To examine the effectiveness of the DFDI scheme, the following six cases are considered as examples to show how the residuals will behave:

- Case 1: All sensors are normally operated with external disturbances applied to the primary mirror.
- Case 2: One sensor is saturated at time 1000 with a value of 5 volts to simulate a real situation when a sensor coil is opened.
- Case 3: Two sensors are failed; sensor 1 is

failed at time 500 with a value of 5 volts, and sensor 2 is failed at time 1000 with a value of 5 volts.

Fig. 3 shows the residual signals for all three cases. In these results, all residuals generated by non-faulty sensor outputs have small values comparing to other residuals generated by the faulty sensor outputs. These residuals are evaluated to find the best threshold values that will reduce the risk of false alarms coming from system noise, external disturbances, subsystem interactions, and modeling errors.

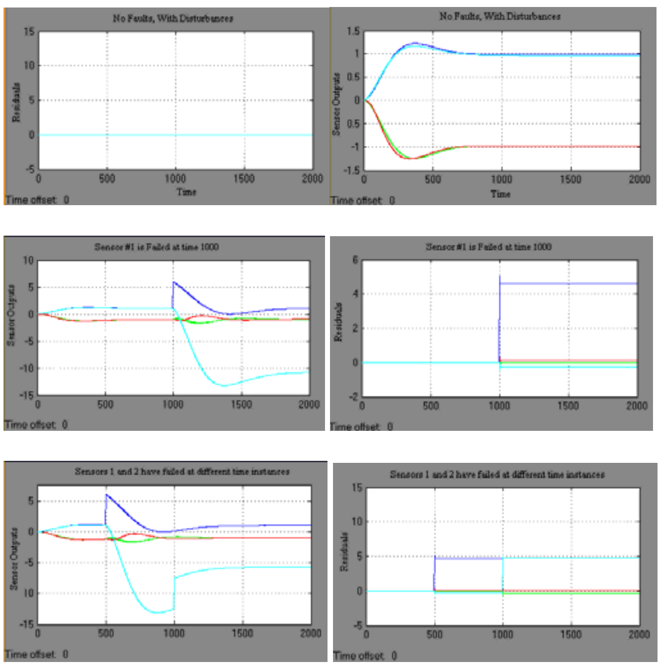

Fig. 3 Residual Signals for all 3 cases

6 Implementation Results

The DFDI algorithm was implemented on the SPACE testbed and tests were run to determine the algorithm's ability to detect faults, as well as its ability to distinguish between faults and disturbances. To examine the effectiveness of the DFDI algorithm on the testbed, the following scenarios were considered:

- Case 1: All sensors operating normally, with no faults or disturbances applied to the system.
- Case 2: All sensors operating normally, with a sudden disturbance applied to the system by manually displacing the panel being observed.
- Case 3: A fault was caused by disconnecting a sensor from the system.

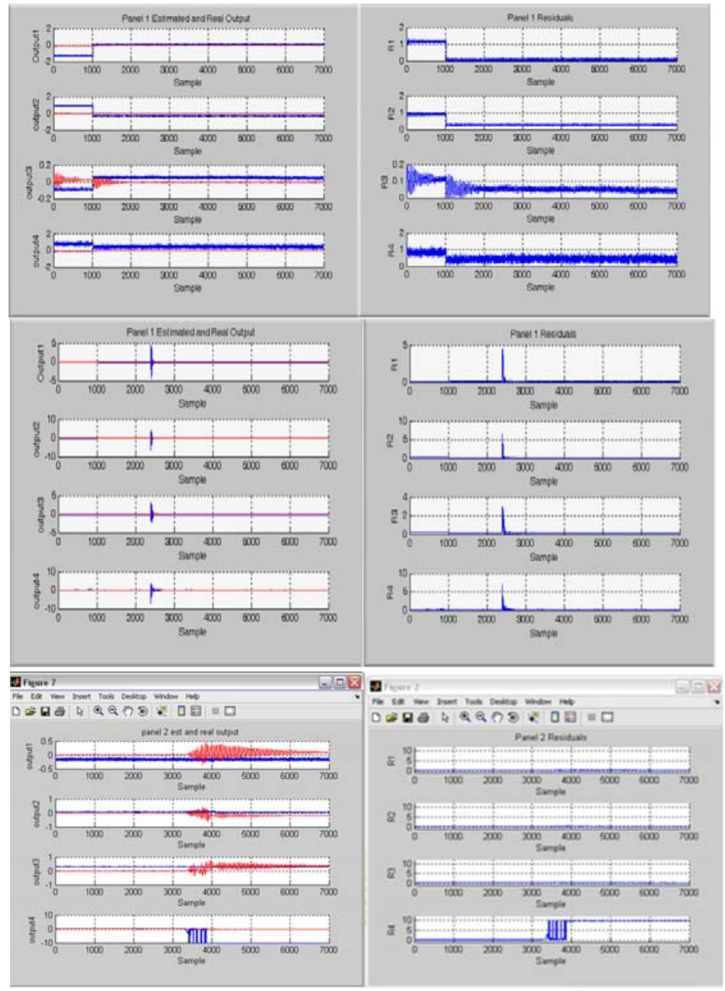

Fig. 4 System real and estimated outputs (left) and residual outputs (right) for all three implementation cases

Fig. 4 shows the results from each of the three cases. In the case where only a disturbance was added, the residuals briefly rose above near zero values before returning to normal. In the faulty case, the results conformed to the simulated signals, with the residual signal from the faulty sensor having a much higher value than the surrounding sensors.

7 Conclusion and Future Work

This paper describes the fault tolerant control challenge related with the SPACE testbed that is located in the Structures, Pointing And Control Laboratory at California State University, Los Angeles. With the DFDI algorithm successfully simulated and implemented, the current task now involves using the DFDI algorithm to develop and implement reconfiguration techniques to realize top level system requirements after component failure.

References

[1] H. S. Stockman, "The Next Generation Space Telescope Visiting a Time When Galaxies Were Young", June 1997.

[2] H. Boussalis, "Decentralization of Large Space borne Telescopes", Proc. 1994 SPIE Symposium on Astronomical Telescopes, Hawaii, 1994.

[3] H. Boussalis, M. Mirmirani, A. Chassiakos, K. Rad, "The Use of Decentralized Control in Design of a Large Segmented Space Reflector", Control and Structures Research Laboratory, California State University, Los Angeles, Final Report, 1996.

[4] P. M. Frank, "Fault Diagnosis in Dynamic Systems Using Analytical and Knowledge-based Redundancy", 1990 International Federation of Automatic Control, vol. 26, pp. 459 – 474, 1990.

[5] M. Hou, P. Zitek, R. J. Patton, "An Observer Design for Linear Time-Delay Systems", IEEE Transactions on Automatic Control, vol. 47, January 2002.

[6] S. H. Wang and E. J. Davison, "On the stabilization of decentralized control systems", IEEE. Transaction on Automatic Control, PP. 473-78, 1973.

[7] E.Y. Chow, A. S. Willsky, "Analytical redundancy and the design of robust failure detection systems," IEEE Transactions on Automatic Control, AC-29, pp. 603-614, 1984.

[8] H. Boussalis, "Stability of Large Scale Systems", New Mexico, USA, November, 1979.

[9] R. J. Patton, "Fault-tolerant control systems: The 1997 situation," in Proc. IFAC Symp. Fault Detection, Supervision and Safety for Technical Processes (SAFEROCESS), pp. 1033-1055, 1997.

[10] D. G. Luenberger, "Observers for Multivariable Systems", IEEE Transactions on Automatic Control, AC-11, pp. 190-197, 1966.